

# Weak Electron Irradiation Suppresses the Anomalous Magnetization of N-Doped Diamond Crystals

Annette Setzer, Pablo D. Esquinazi,\* Olesya Daikos, Tom Scherzer, Andreas Pöppl, Robert Staacke, Tobias Lühmann, Sebastien Pezzagna, Wolfgang Knolle, Sergei Buga, Bernd Abel, and Jan Meijer

Several diamond bulk crystals with a concentration of electrically neutral single substitutional nitrogen atoms of  $\lesssim 80$  ppm, the so-called C or P1 centers, are irradiated with electrons at 10 MeV energy and low fluence. The results show a complete suppression of the irreversible behavior in field and temperature of the magnetization below 30 K, after a decrease in  $\lesssim 40$  ppm in the concentration of C centers produced by the electron irradiation. This result indicates that magnetic C centers are at the origin of the large hysteretic behavior found recently in nitrogen-doped diamond crystals. This is remarkable because of the relatively low density of C centers, stressing the extraordinary role of the C centers in triggering those phenomena in diamond at relatively high temperatures. After annealing the samples at high temperatures in vacuum, the hysteretic behavior is partially recovered.

determine the metallic character of the heavily boron-doped superconducting diamond.<sup>[4]</sup> Meanwhile, there are indications of SC below 12 K in B-doped carbon nanotubes,<sup>[5]</sup> at  $\approx 25$  K in heavily B-doped diamond samples<sup>[6]</sup> or even at  $\approx 55$  K in 27% B-doped Q-carbon, an amorphous form of carbon.<sup>[7]</sup> In spite of several experimental and theoretical studies on the influence of boron as a trigger of SC in diamond and in some carbon-based compounds, the real role of boron and the origin of SC in diamond is not so clear as it may appear. For example, scanning tunneling microscopy studies of superconducting B-doped polycrystalline diamond samples revealed granular SC with an unclear boron concentration within the superconducting

regions.<sup>[8]</sup> In spite of an apparently homogeneous boron concentration, strong modulation of the order parameter was reported in the study by Zhang et al.,<sup>[8]</sup> putting into question the real role of boron in the SC of diamond. High-resolution structural studies accompanied by electron energy loss spectroscopy (EELS) on B-doped diamond single crystals revealed the presence of boron in distorted regions of the diamond lattice inducing the authors to argue that SC may appear in the disordered structure and not in the defect-free B-doped lattice of diamond.<sup>[9]</sup> This peculiarity may explain the high sensitivity of the superconducting critical


## 1. Introduction

### 1.1. Superconductivity in Diamond: a Still Incomplete Puzzle

Superconductivity (SC) was recognized in doped diamond through a relatively broad transition in the electrical resistance at 2.5–2.8 K after doping it with  $\approx 3\%$  boron.<sup>[1,2]</sup> A critical temperature onset of 8.7 K was reported in polycrystalline diamond thin films 1 year later.<sup>[3]</sup> Angle-resolved photoemission spectroscopy (ARPES) studies revealed that holes in the diamond bands

A. Setzer, P. D. Esquinazi  
Division of Superconductivity and Magnetism  
Felix-Bloch Institute for Solid State Physics  
Universität Leipzig  
Leipzig 04103, Germany  
E-mail: esquin@physik.uni-leipzig.de

O. Daikos, T. Scherzer, W. Knolle, B. Abel  
Leibniz Institute of Surface Engineering (IOM)  
Leipzig 04318, Germany

 The ORCID identification number(s) for the author(s) of this article can be found under <https://doi.org/10.1002/pssb.202100395>.

© 2021 The Authors. physica status solidi (b) basic solid state physics published by Wiley-VCH GmbH. This is an open access article under the terms of the Creative Commons Attribution-NonCommercial License, which permits use, distribution and reproduction in any medium, provided the original work is properly cited and is not used for commercial purposes.

DOI: 10.1002/pssb.202100395

A. Pöppl  
Division of NMR  
Felix-Bloch Institute for Solid State Physics  
Universität Leipzig  
Leipzig 04103, Germany

R. Staacke, T. Lühmann, S. Pezzagna, J. Meijer  
Division of Applied Quantum Physics  
Felix-Bloch Institute for Solid State Physics  
Universität Leipzig  
Leipzig 04103, Germany

S. Buga  
Technological Institute for Superhard and Novel Carbon Materials  
Troitsk, Moscow 108840, Russia

S. Buga  
Moscow Institute of Physics and Technology  
Dolgoprudny, Moscow Region 141701, Russia

current between hydrogen- and oxygen-terminated boron-doped diamond.<sup>[10]</sup>

Furthermore, we may ask whether the SC phase in B-doped diamond is homogeneously distributed in the reported samples. This does not appear to be in general the case. For example, the SC phase was observed only within a near surface region of less than  $\approx 1 \mu\text{m}$  in heavily B-doped diamond single crystals, showing clear polycrystallinity and granular properties.<sup>[11]</sup> Some studies associated the Mott transition observed as a function of the B concentration with metallic B–C bilayers; the measured SC was detected at the surface of the doped crystals having a short modulation period between the B–C bilayers.<sup>[12]</sup> Apparently, differences in the growth processes of the diamond samples cause differences in the morphology of the SC phase, an issue that still needs more studies.

Several recent studies indicate a granular nature of the samples' structure and of the SC phase.<sup>[12–15]</sup> The granular nature of the SC phase and localized disorder may play an important role as recently reported experimental facts indicate, namely: a) not always there is a clear correlation between the B-concentration threshold for the metal–insulator transition and the one for SC,<sup>[16]</sup> and b) there is no simple dependence between the free-carrier concentration and the critical temperature characterized by transport measurements.<sup>[17]</sup>

Another open issue in the SC puzzle of doped diamond is the fact that implanting boron into diamond via irradiation does not trigger SC at least above 2 K.<sup>[18]</sup> It has been argued that this irradiation process does not trigger SC because of the produced defects that remained in the diamond lattice after ion irradiation. However, this is not at all clear because the sample was heated to 900 °C during irradiation and afterward annealed at 1700 °C in vacuum,<sup>[18]</sup> see also similar results in the studies by Willems van Beveren et al. and Tsubouchi et al.<sup>[19–21]</sup> It might be that the absence of SC in the irradiated samples after high temperature annealing is related to the absence of certain defects and not other way around.<sup>[22]</sup> That certain lattice defects are of importance for SC can be seen from the reentrance of SC observed in ion-irradiated B-doped diamond after high-temperature annealing.<sup>[17]</sup> This reentrance of SC has been attributed to the partial removal of vacancies previously produced by light ion irradiation. It has been argued that vacancies change the effective carrier density compensating the boron acceptors and therefore suppressing SC.<sup>[17]</sup>

## 1.2. Defect-Induced Phenomena and the Unconventional Magnetization Observed in Nitrogen-Doped Diamond Crystals

According to recent studies, the reported SC in B-doped diamond appears to be more complicated because not only the boron concentration matters but also some kind of disorder or even magnetic order may play a role. Coexistence of SC and ferromagnetism (FM) was recently reported in hydrogenated B-doped nanodiamond films at temperatures below 3 K.<sup>[23,24]</sup> Earlier studies<sup>[25]</sup> showed the existence of ferromagnetic hysteresis at room temperature in the magnetization of nanodiamonds after nitrogen or carbon irradiation. Recently published studies revealed the existence of large hysteresis in field and temperature in the magnetization below an apparent critical temperature

$T_c \approx 30 \text{ K}$  in B-free bulk diamond single crystals. Those crystals were produced under high-temperature and high-pressure (HTHP) conditions with an average N-concentration  $\lesssim 100 \text{ ppm}$ .<sup>[26]</sup> In this last work, a correlation was found between the strength of the hysteretic behavior in the magnetization with the N content, in particular, with the concentration of C centers.

We would like to stress that the possible origins for an irreversible behavior in field and/or temperature in the magnetization of a material can be: a) intrinsic magnetic anisotropy, b) the existence of magnetic domains and the pinning of their walls, or c) the pinning of vortices or fluxons in a superconducting matrix. The origin (a) can be ruled out because the measured behavior does not depend on the direction of the applied field with respect to the main axes of the crystals nor on their shape.<sup>[26]</sup> This independence has been confirmed once more in the diamond crystals studied in this work.

The relatively low average N content and further details of the measured diamond samples suggest the existence of a granular structure in the concentration of nitrogen.<sup>[26]</sup>

To facilitate the comparison of the present results with those in the study by Barzola-Quiquia et al.,<sup>[26]</sup> we give a summary of the main results obtained from the measurements of eight different nitrogen-doped crystals: a) All samples with nitrogen concentration below 120 ppm show unconventional magnetic moment behavior in the field hysteresis and temperature dependence below  $\approx 30 \text{ K}$ . As example, we show in **Figure 1**, the field hysteresis of one of the measured samples in this study, before and after annealing. Above  $\approx 30 \text{ K}$  all samples behave as a typical undoped diamagnetic diamond. b) The irreversible magnetization of the diamond samples can be phenomenologically understood as the superposition of a diamagnetic, superparamagnetic (SPM) (or ferromagnetic), and superconducting contributions. We stress that the main characteristics of the anomalous hysteresis are also observed in ferromagnetic/superconducting oxide

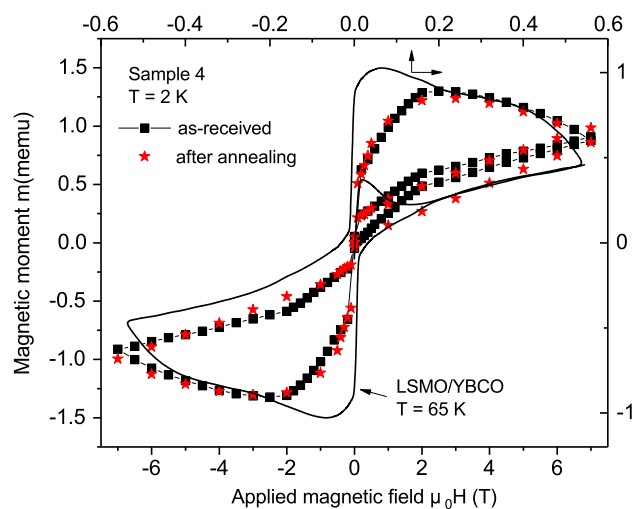


**Figure 1.** Left-bottom axes: Magnetic field hysteresis loop at  $T = 2 \text{ K}$  of the magnetic moment of sample 4 studied in this work, before and after annealing 4 h at 1200 °C in vacuum. Right-upper axes: ferromagnetic/superconducting  $\text{La}_{2/3}\text{Sr}_{1/3}\text{MnO}_3/\text{YBa}_2\text{Cu}_3\text{O}_{7-x}$  (LSMO/YBCO) bilayer at 65 K taken from the study by Barzola-Quiquia et al.<sup>[26]</sup> A small diamagnetic linear field background was subtracted from the data points.

bilayers for fields applied parallel to the main area (and interface between) of the two layers, see Figure 1. More hysteresis loops can be seen in the study by Barzola-Quiquia et al.<sup>[26]</sup> and in its supplementary information. The similarities in the minutest details between the field loops obtained at different temperatures starting both in the virgin, zero field cooled states, are striking. Note that, we are comparing two data sets with very similar absolute magnetic moments using the same SQUID magnetometer. The strength of the magnetic moment signal does indicate that we are dealing with a huge effect, 5 orders of magnitude larger than the sensitivity of our SQUID magnetometer (of the order of  $10^{-8}$  emu). The similarities in the field hysteresis and also in the temperature dependence of the magnetic susceptibility suggest the existence of superparamagnetic and superconducting regions in the N-doped diamond crystals. c) The amplitude of the anomalous magnetization signal below  $\approx 30$  K increases with the nitrogen-related C-center concentration. d) The obtained phase diagrams for both phases found in the N-doped diamond samples below 30 K indicate that the ordering phenomena should have a common origin. In contrast to the amplitude of the anomalous magnetization, the critical temperature—below which the hysteretic behavior is measured—does not depend significantly on the C-center concentration. This result suggests that localized C-center clusters with similar C-center concentration trigger the anomalies below 30 K. e) The magnetic and superconducting regions are of granular nature embedded in the dielectric diamond matrix. The used Bean-like model to fit the field hysteresis suggests the existence of superconducting shielding currents and field gradients within the grains of size larger than a few nanometers. f) The total mass of the regions of the samples that originates the anomalous magnetization behavior was estimated as  $\approx 10^{-4}$  of total sample mass, emphasizing its granular nature and the difficulties one has to localize them in large bulk samples.

We note that nitrogen, as a donor impurity in diamond, is expected to trigger SC with higher critical temperatures than with boron.<sup>[22]</sup> This prediction is based on the higher binding energy of substitutional nitrogen in diamond, in comparison to boron. However, if one takes boron as example, a nitrogen concentration of a few percent appears to be experimentally difficult to achieve in equilibrium conditions. Therefore, it has been argued that disorder or defective regions and an inhomogeneous N concentration in the diamond lattice may play a role in triggering granular SC.<sup>[22]</sup>

Interestingly, compression-shear deformed diamond was recently proposed as a new way to trigger phonon-mediated SC up to 12 K in undoped diamond.<sup>[27]</sup> Defect-induced SC is actually not a new phenomenon but was already reported in different compounds. For example, strain-induced SC at interfaces of semiconducting layers has been treated theoretically based on the influence of partial flat-bands.<sup>[28]</sup> SC was found in semiconducting superlattices up to 6 K and attributed to dislocations<sup>[29]</sup> at the interfaces.<sup>[30]</sup> Furthermore, SC was discovered at artificially produced interfaces in Bi and BiSb bicrystals having a  $T_c \lesssim 21$  K, whereas neither Bi nor BiSb are superconducting.<sup>[31]</sup> Finally, SC at 2D interfaces has been recently studied at the stacking faults of pure graphite or multilayer graphene structures theoretically<sup>[32–34]</sup> and experimentally.<sup>[35,36]</sup>

### 1.3. Aims of This Work

Because of the large penetration depth at the selected electron energy, we use a weak electron irradiation to study the influence of lattice defects produced or changed by the irradiation on the magnetization of bulk N-doped diamond crystals. Weak electron irradiation means that its fluence is of the order of the concentration of C centers, i.e., a few tens of ppm. Magnetization measurements can provide valuable information especially in the case the phase(s) at the origin of the anomalies of interest, is (are) not homogeneously distributed in the samples. One aim of this work is therefore to check with temperature- and field-dependent measurements of the magnetization, whether its anomalous behavior found in N-doped diamond crystals can be affected by a weak electron irradiation.

If the irradiation does change the anomalies observed in the magnetization, which lattice defect is mostly affected by the irradiation? Can it be correlated to the magnetic anomalies? A recently published study on the influence of ion irradiation on the SC of heavily B-doped diamond samples, showed that SC is suppressed after He-ion irradiation of  $5 \times 10^{16}$  at 1 MeV producing a vacancy concentration of  $\approx 3 \times 10^{21} \text{ cm}^{-3}$  ( $\approx 2\%$ ).<sup>[17]</sup> This apparent complete suppression of SC after irradiation was experimentally observed by electrical resistance measurements. Therefore, we may further ask, if the nominal concentration of produced vacancies by the irradiation that affects the magnetic properties is also of the order of the C-center concentration. Furthermore, can a high-temperature annealing in vacuum of the irradiated samples recover the anomalous behavior in the magnetization?

## 2. Experimental Section

### 2.1. Samples and Characterization Methods

We selected four (111) diamond bulk crystals, three of them were previously studied in detail.<sup>[26]</sup> The N-doped diamond single crystals were obtained from the Japanese company Sumitomo. The crystals were cleaned with acid (boiling mixture of nitric acid (100%), sulfuric acid (100%), and perchloric acid (70%) with a mixing ratio of 1:3:1 for 4 h). All four “as-received” samples were cleaned before any measurement was started. The presence of magnetic impurities was characterized by particle induced X-ray emission (PIXE) with ppm resolution in a diamond sample with similar magnetic characteristics as the samples we used in this study.<sup>[26]</sup> The PIXE results indicated an overall impurity concentration below 10 ppm with a boron concentration below the resolution limit of 1 ppm. Table 1 shows further characteristics of the samples.

Because of the dielectric properties of the diamond matrix, we are actually rather restricted to measure the magnetic moment of the samples to characterize their magnetic response as a function of field and temperature. Even after irradiation the samples remain highly insulating, although their yellow color gets opaque. The magnetic moment of the samples was measured using a superconducting quantum interference device magnetometer (SQUID) from Quantum Design. Due to the expected granularity of the phases responsible for the anomalous behavior of the

**Table 1.** Measured samples with their main characteristics and treatments. (★): These samples were previously characterized in the study by Barzola-Quiquia et al.<sup>[26]</sup> The concentration of PM centers from SQUID measurements was obtained from the linear slope of the magnetic susceptibility versus  $1/T$  assuming  $J = 1/2$  and  $g_j = 2$  and has an experimental error  $\lesssim \pm 7$  ppm. The error of the average C center concentration obtained from EPR is  $\approx 15\%$ . The written range of the C centers concentrations (error  $\lesssim 5\%$ ) obtained from IR-absorption spectroscopy represents the minimum and maximum concentrations measured at different locations of the same sample, an indication of the inhomogeneous N-distribution. The electron irradiation was carried out in vacuum and at  $900^\circ\text{C}$ . Each annealing treatment was 4 h in vacuum at  $1200^\circ\text{C}$  with a heating and cooling time of 10 h.

	Name	Size [mm <sup>3</sup> ]	Mass [mg]	PM [ppm] (SQUID)	C [ppm] (EPR)	C [ppm] (IR)	Treatment
1	CD2318-02	$2.4 \times 2.4 \times 1.7$	34.1	–	40	33...47	as-received
2	CD2318-01★	$2.4 \times 2.4 \times 1.7$	34.0	–	–	60...65	as-received
				80	20	15...27	e <sup>−</sup> -irrad. ( $2 \times 10^{18} \text{ cm}^{-2}$ )
				76	–	13...25	annealed
3	CD1512-02★	$1.6 \times 1.5 \times 1.2$	9.8	–	–	18...25	as-received
				40	–	–	e <sup>−</sup> -irrad. ( $1 \times 10^{18} \text{ cm}^{-2}$ )
				39	10	5...10	annealed
				44	–	–	annealed
4	CD2520★	$2.5 \times 2.5 \times 2$	44.1	–	–	26...40	as-received
				–	–	–	annealed

magnetization, local magnetic measurements (MFM or micro-Hall sensors, as example) are certainly of interest and in principle possible. However, assuming that the phases of interest are at the near surface region, the relatively large area of the samples (some mm<sup>2</sup>, see Table 1) makes local measurements time consuming, typically several months for an area of 1 mm<sup>2</sup> and at a given temperature and magnetic field.

As in the study by Barzola-Quiquia et al.,<sup>[26]</sup> the presence of regions with internal stress was investigated by polarized light microscopy. Within experimental resolution those regions were not significantly changed after electron irradiation.

Continuous wave (CW) electron paramagnetic resonance (EPR) measurements were carried out at room temperature with a Bruker EMX Micro X-band spectrometer at 9.416 GHz using a Bruker ER 4119HS cylindrical cavity. Absolute concentrations of paramagnetic (PM) C centers (usually called P1 centers in EPR) and NV<sup>−</sup> centers were determined in dark by using an ultramarine standard sample with known spin number and double integration of the corresponding EPR spectra. The external magnetic field  $B_0$  was oriented along the [111] crystallographic axis of the diamond single crystals. In order to avoid saturation effects a 10 kHz modulation frequency at a microwave (MW) power of  $P_{\text{MW}} = 630$  nW was used. We verified that the EPR signal intensities  $I_{\text{EPR}}$  of both centers deviate from a square root dependence on  $P_{\text{MW}}$  by less than 10% between  $P_{\text{MW}} = 203$  and 630 nW and therefore saturation effects can be neglected at room temperature and such low MW power levels. Modulation amplitudes of 0.1 and 0.03 mT were used to measure the C- and NV<sup>−</sup> centers to avoid broadening effects.

A reliable method to characterize the granular, inhomogeneous concentration of nitrogen and the N-based centers, like the C centers (neutral nitrogen N<sup>0</sup> with a maximum absorption at  $1344 \text{ cm}^{-1}$ ) and N<sup>+</sup> (positively charged single substitutional nitrogen with a maximum absorption at  $1332 \text{ cm}^{-1}$ ), is infrared (IR) microscopy. IR measurements and IR spectral imaging were carried with a Hyperion 3000 IR microscope coupled to a Tensor

II FTIR spectrometer (Bruker Optik GmbH, Ettlingen, Germany). The microscope was equipped with both, a single element MCT detector and a  $64 \times 64$  pixel focal plane array (FPA) detector. Measurements with the mercury cadmium telluride (MCT) detector were carried out with a spectral resolution of  $1 \text{ cm}^{-1}$ , whereas the resolution of the FPA detector used for imaging was limited to  $4 \text{ cm}^{-1}$ . Diamonds were fixed in a Micro Vice sample holder (S.T. Japan) and carefully aligned horizontally.

The concentration values of C centers shown in Table 1 were obtained from IR transmission spectra taken with the MCT detector at various positions of the diamond surface. The MCT detector was favored over the FPA detector for these measurements due to the very low bandwidths of the aforementioned bands. Quantitative concentration data of N<sup>+</sup> and C centers were derived from the spectra using the relationships between the peak intensities of these bands and the concentration of corresponding nitrogen centers given by Lawson et al.,<sup>[37]</sup> see Section 4.

## 2.2. Electron Irradiation

Electron irradiation was done at 10 MeV energy using a B10-30MPx Mevex Corp. (Stittsville, Canada) with a total irradiation fluence of  $1 \times 10^{18}$  electrons cm<sup>−2</sup> (sample 3) and  $2 \times 10^{18}$  electrons cm<sup>−2</sup> (sample 2). The electron irradiation was carried out at  $900^\circ\text{C}$  in vacuum, in order to remove a certain amount of disorder. In spite of a large number of studies on irradiation effects in diamond, the available literature on the electron irradiation damage in diamond is less extensive. For example, electron irradiation at high temperatures was used to significantly increase the density of nitrogen–carbon vacancy (NV) centers.<sup>[38,39]</sup> Several characteristics of the electron irradiation damage in diamond were published by Campbell and Mainwood.<sup>[40]</sup> From that study, we estimate a maximum penetration depth of



$\approx 15$  mm at the used electron energy. This indicates that the irradiated electrons completely penetrate the used samples.

There are two recent works directly related to our studies. One of them investigated the effects of electron irradiation on in situ heated nanoparticles of diamond.<sup>[41]</sup> These samples were irradiated with the same accelerator as our crystals. In the study by Capelli et al.,<sup>[39]</sup> the authors increased the NV-center concentration through electron irradiation maintaining the bulk diamonds at high temperatures. Both studies showed a higher conversion rate of C centers into NVs with in-situ annealing. Considering those studies, we used 10 MeV electrons irradiation to convert C centers into NVs. The selected fluences were chosen to produce a nominal concentration of vacancies similar to the concentration of magnetic C centers existent before irradiation. In this way, we can directly check, whether a change in the concentration of C centers affects or not, the magnetization of our samples.

In terms of created vacancies, homogeneously induced by the electron irradiation, the maximal nominal concentration would be  $5 \times 10^{18} \text{ vac. cm}^{-3}$  for sample 3, i.e., a concentration of  $\approx 30$  ppm (60 ppm for sample 2), of the same order as the C centers obtained by IR and EPR, see Table 1. Obviously, the vacancy concentration that remains in the samples is smaller because of the high temperature of the samples during the irradiation process.<sup>[42]</sup> It means that some of the vacancies can give rise to N-related defects and others diffuse to the sample surface. From the change in the concentration of NV centers one can estimate the vacancy concentration that remains.

### 3. Electron PM Resonance

Figure 2 shows EPR spectra of the diamond single crystal samples 1 and 2 recorded for  $\mathbf{B}_0 \parallel [111]$ . Both samples show the intense signals of the C donor of nitrogen incorporated at carbon lattice sites having an electron spin  $S = 1/2$  and the typical  $^{14}\text{N}$  hyperfine (hf) splitting into three lines (Figure 2a).<sup>[43]</sup> For the chosen orientation of the single crystals, the external magnetic field  $\mathbf{B}_0$  points along the  $C_3$  symmetry axis of one of the four magnetically nonequivalent C sites in the diamond lattice.<sup>[44]</sup> The  $C_3$  symmetry axis of the C centers defines the symmetry axes of its axially symmetric  $g$  and  $^{14}\text{N}$  hf coupling tensor. The two outer hf lines at 331.8 and 339.9 mT together with the central hf line at 335.8 mT belong to this orientation of the C centers. The symmetry axes of the other three sites of the C centers make an angle of  $109.47^\circ$  with  $\mathbf{B}_0$  and lead to hf lines at 332.8 and 338.9 mT in addition to the central hf line at 335.8 mT. Sample 3 showed a comparable spectrum of the C centers. The concentrations of the C centers in the three diamond single crystal samples 1, 2, and 3 (Table 1) were determined by double integration of the full EPR spectrum considering the quality factor of the cavity and comparison with an ultramarine standard sample with known spin number. We emphasize that the concentration of C centers obtained with this method is similar to the one obtained by IR spectroscopy, see Table 1 and next section.

A broader magnetic field scan with a larger amplification as done for sample 2 (Figure 2b) revealed additional signals of the  $\text{NV}^-$  centers with  $S = 1$ .<sup>[43]</sup> Note that, the intense signals at about 336 mT in Figure 2b are due to C centers. The  $\text{NV}^-$  centers has been assigned to a nitrogen atom substituting a

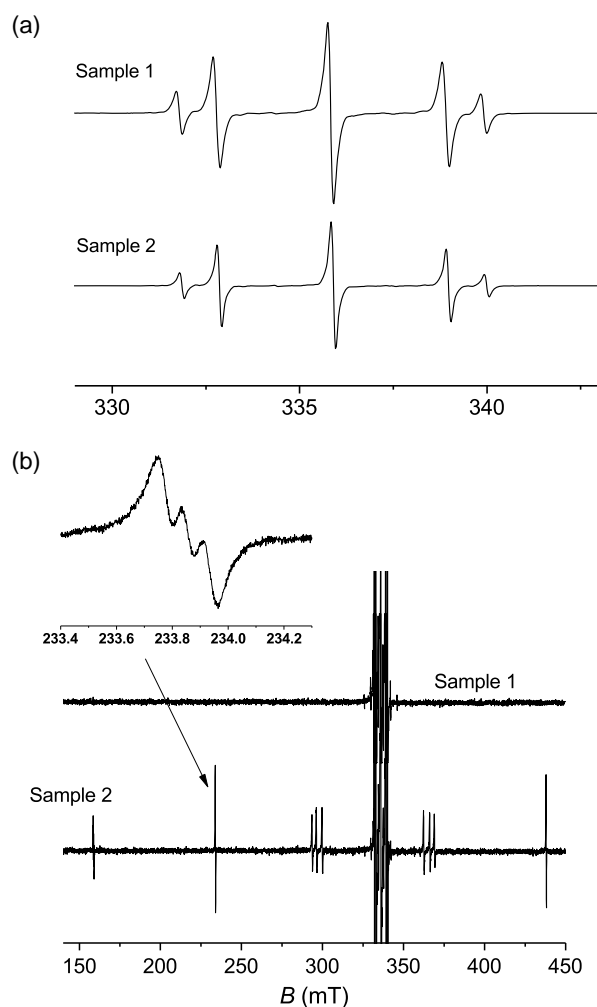


**Figure 2.** EPR spectra obtained at room temperature of samples 1 (as-received) and 2 (after irradiation), see Table 1, for  $\mathbf{B}_0 \parallel [111]$  showing the signals from: a) C centers and b) from  $\text{NV}^-$  centers. The spectra of the  $\text{NV}^-$  centers were recorded with a tenfold higher receiver gain. The insert in (b) displays the  $^{14}\text{N}$  hf splitting of the  $m_S = +1 \leftrightarrow 0$  signal of the  $\text{NV}^-$  centers at 233.8 mT.

carbon lattice site, which is associated with a next neighbored carbon vacancy.  $\text{NV}^-$  centers could not be observed for sample 1. The  $C_3$  symmetry axis of the  $\text{NV}^-$  centers is oriented along the [111] direction and determines the symmetry axis of the axially symmetric zero field splitting tensor of this centers. In samples 2 and 3, the concentration of  $\text{NV}^-$  centers is  $\approx (2 \pm 0.3)$  ppm. Therefore, we assume that these centers do not play any role in the phenomena we discuss in this work.

### 4. IR Spectroscopy

In a first published study of similar diamond crystals, a correlation between the magnitude of the anomalous magnetization below 30 K and the C centers was found.<sup>[26]</sup> Therefore, we characterized the concentration and the space distribution of this magnetic defect. The characterization of this centers in diamond using

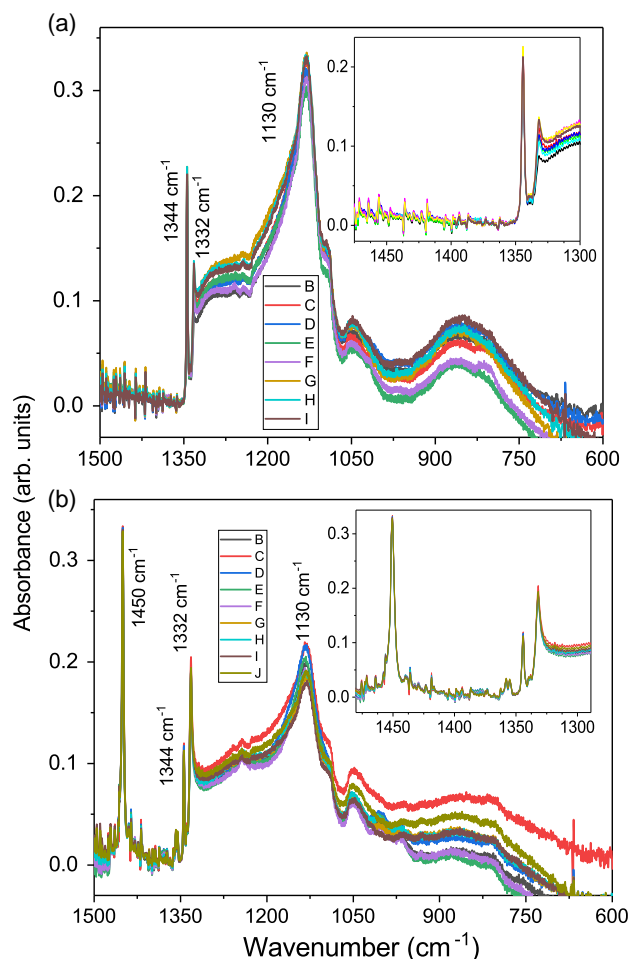


**Figure 3.** a) Infrared spectra of the absorbance versus wavenumber of sample 1 in the as-received state measured in transmission with a resolution of  $1\text{ cm}^{-1}$ . The inset shows a blow out at the high wavenumber region. b) Similar for sample 2 after electron irradiation. The different curves (B ... J) in both figures were obtained at different positions of the sample.

IR spectroscopy has been reported in several earlier studies,<sup>[37,45–47]</sup> including radiation damage and subsequent annealing.<sup>[48]</sup> The C centers are responsible for the broad absorption peak at  $1130\text{ cm}^{-1}$  followed by a very sharp absorption maximum at  $1344\text{ cm}^{-1}$ , see **Figure 3**. The broad one at  $1130\text{ cm}^{-1}$  is attributed to a quasi-local vibration at single substitutional nitrogen atoms,<sup>[37,46,47,49]</sup> whereas the one at  $1344\text{ cm}^{-1}$  is due to a local mode of vibration of the carbon atom at the C–N bond with the unpaired electron.<sup>[50]</sup>

The concentration range of C centers determined from IR spectra and measured at different positions of the samples is shown in Table 1. The values were obtained using the relationship  $C\text{ (ppm)} = 37.5 A_{1344\text{cm}^{-1}}^{[37]}$  where  $A_{1344\text{cm}^{-1}}$  is the peak intensity at the corresponding wavenumber. The concentration range of  $\text{N}^+$  centers can be estimated from the absorption peak at  $1332\text{ cm}^{-1}$  (using  $\text{N}^+\text{ [ppm]} = 5.5 A_{1332\text{cm}^{-1}}^{[37]}$ ). In all samples and states of the samples, the  $\text{N}^+$  concentration is much smaller (factor 3–10) than the C centers concentration and therefore it will not be considered in the discussion of the results. We note that the range of C centers

concentration obtained from IR absorption agrees very well with the average concentration obtained from EPR, see Table 1.

As example, **Figure 3** shows the IR spectra of: a) sample 1 in the as-received state and b) sample 2 after electron irradiation. All spectra were obtained in transmission (MCT detector) with a resolution of  $1\text{ cm}^{-1}$  at different positions of the sample surface. After electron irradiation, a new maximum at  $1450\text{ cm}^{-1}$  appears, see **Figure 3b**. We note that in the as-received state of all samples this maximum is absent within experimental resolution, see **Figure 3a** as example.

The maximum absorption at  $1450\text{ cm}^{-1}$  was already shown to develop during the annealing at  $T > 500^\circ\text{C}$  in type I diamonds after electron irradiation and is related to N interstitials in the diamond lattice.<sup>[51]</sup> Since then, it has been studied and reported several times.<sup>[52–54]</sup> Last published characterization measurements indicate that the origin of this maximum is related to H1a centers (dinitrogen interstitials).<sup>[53,54]</sup> The vanishing or growth of H1a centers appears to be correlated to the interplay between C- and  $\text{N}^+$ -center aggregation processes. The results in the study by Babich et al.<sup>[54]</sup> suggest that an increase in the density of H1a centers is accompanied by a decrease in the density of C centers.

To quantitatively estimate the extent of the increase in the concentration of H1a centers [H1a], we use a relation given by Dale,<sup>[55]</sup> which relates the band integral  $A$  at  $1450\text{ cm}^{-1}$  to the concentration of interstitials according to  $[\text{H1a}]\text{ (ppm)} = A\text{ (in cm}^{-1}\text{)}/f$ , with  $f = 3.4 \times 10^{-17}\text{ cm}$ . Spectra taken with the MCT detectors at various positions of the irradiated diamond before and after annealing were baseline-corrected and normalized according to the study by Dale<sup>[55]</sup> before conversion of the band integrals to [H1a]. Finally, the individual values of [H1a] were averaged. Using this procedure for the results of sample 2, we found a slight increase in [H1a] from  $\approx 3\text{ ppm}$  before annealing to  $\approx 3.3\text{ ppm}$  after annealing. The values indicate that  $[\text{H1a}] \lesssim 15\%$  of the C-center concentration.

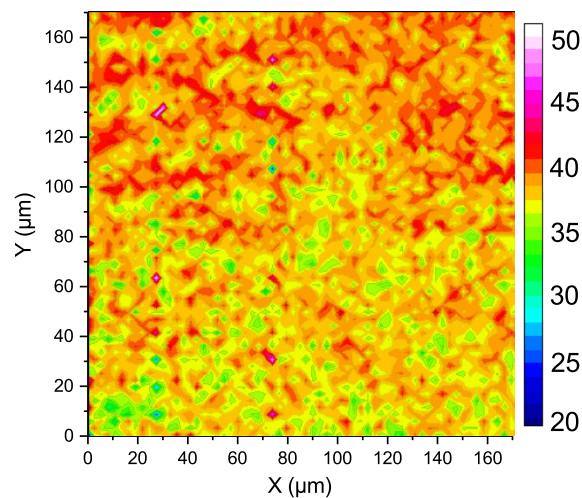


**Figure 4.** Distribution of C centers in an area of  $(170 \times 170)\text{ }\mu\text{m}^2$  of sample 1, obtained from the maximum intensity of the IR band at  $1344\text{ cm}^{-1}$  using a FPA detector with a resolution of  $4\text{ cm}^{-1}$ . The color scale indicates the concentration of C centers in ppm. Note that, this 2D distribution is the sum of the whole absorption through the whole sample thickness at the selected energy. The concentration values in the color scale are in ppm.

Because the concentration of C centers plays a main role in the origin of the phenomena observed in the magnetization, it is of interest to display the concentration distribution of these centers. **Figure 4** shows one example of this distribution measured in sample 1 (as-received state) recorded in transmission with the FPA detector, i.e., the image accounts for the absorption around  $1344\text{ cm}^{-1}$  measured through the whole sample thickness with a spectral resolution of  $4\text{ cm}^{-1}$ . This image shows a remarkable granular-like distribution of the concentration in the selected area of  $170 \times 170\text{ }\mu\text{m}^2$ . This image indicates the existence of regions of a few  $\mu\text{m}^2$  with clear differences in the concentration of C centers of up to  $\approx 25\%$  between some neighboring regions, see **Figure 4**. According to the IR absorption peak at  $1344\text{ cm}^{-1}$ , the concentration of C centers can reach values up to  $\approx 50\text{ ppm}$  locally, depending on the region of the sample.

**Figure 5** shows the concentration distribution of C centers of sample 2 after electron irradiation (**Figure 5a**) and subsequent annealing (**Figure 5b**), see also **Table 1**, both measured at the same sample area. The distribution of the H1a centers correlated to the maximum at  $1450\text{ cm}^{-1}$ , after electron irradiation (**Figure 6a**) and after subsequent annealing (**Figure 6b**) at the same sample area, is shown in **Figure 6**.

Several details are of interest, namely: 1) the average concentration of C centers after electron irradiation decreases

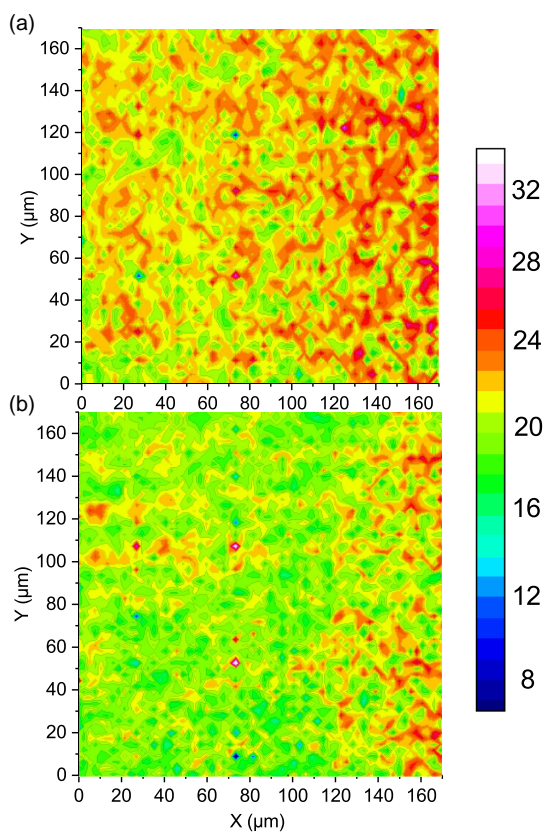


**Figure 5.** Distribution of C centers in an area of  $(170 \times 170)\text{ }\mu\text{m}^2$  of sample 2: a) after electron irradiation and b) after annealing measured at the same location using a FPA detector with a resolution of  $4\text{ cm}^{-1}$ . Data were obtained from the maximum intensity of the IR band at  $1344\text{ cm}^{-1}$ . The color scale indicates the concentration of C centers in ppm.

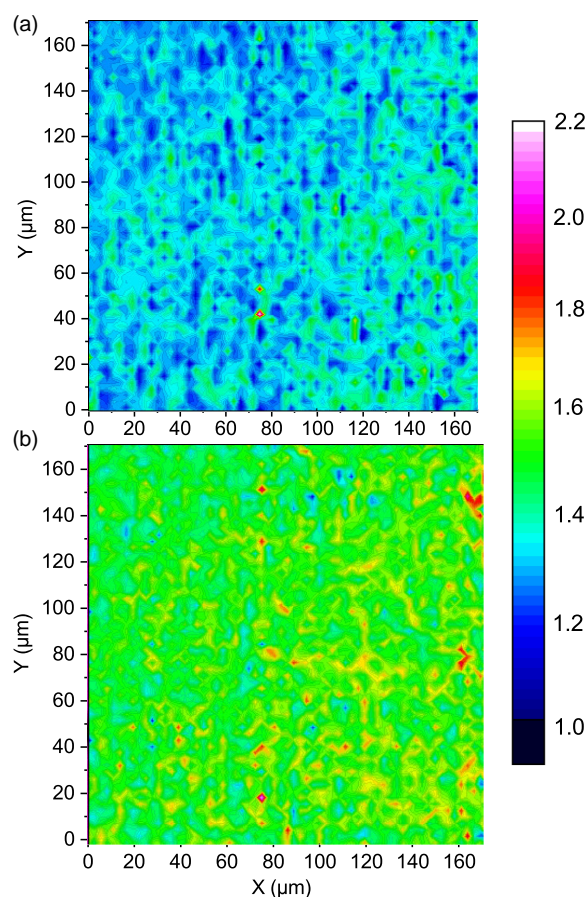


**Figure 6.** Similar to **Figure 4** and **5** but for the IR absorption at  $1450\text{ cm}^{-1}$  due to H1a centers of sample 2: a) after electron irradiation and b) after annealing. The color scale indicates the amplitude of the absorption maximum at  $1450\text{ cm}^{-1}$ . To approximately estimate the concentration in ppm, multiply the numbers at the color scale by two.

by  $\approx 50\%$  and shows a similar granular distribution as in the as-received samples but with a larger difference (up to 50%) between neighboring regions. 2) After annealing, see **Figure 5b**, the average concentration of C centers decreases further by  $\approx 6\%$  but shows a more homogeneous distribution, see also **Table 1**. 3) The concentration of H1a centers (see **Figure 6**), which appear only after irradiation and annealing,<sup>[51]</sup> becomes homogeneously distributed and its average density increases by  $\approx 10\%$  after annealing.

## 5. Magnetization Results

### 5.1. Field Hysteresis Loops

The field hysteresis loops were measured at constant temperature after zero field cooling (ZFC) from 380 K. The field was swept from  $0\text{ T} \rightarrow +7 \rightarrow -7\text{ T} \rightarrow +7\text{ T}$ . After this procedure, the applied field was set to zero, the sample heated to 380 K and cooled at zero field to a new constant temperature. The main characteristics of the anomalous hysteresis at 2 K is shown in **Figure 1** and **7**, observed in all samples before irradiation.



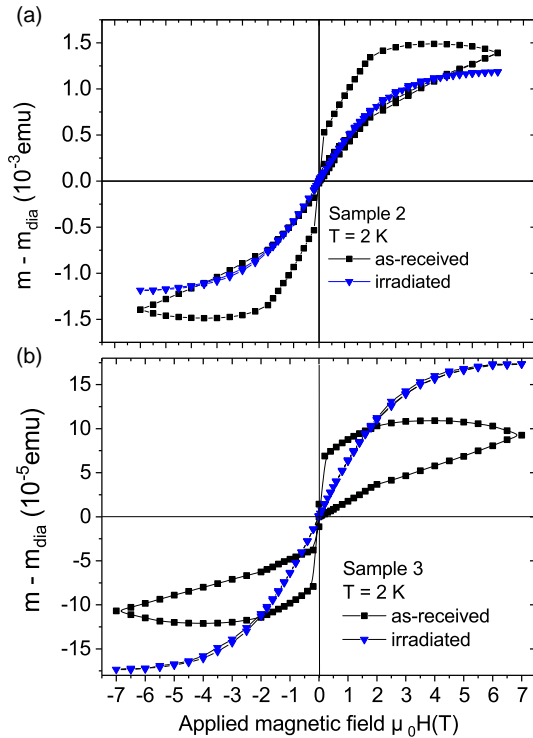


**Figure 7.** Field hysteresis loops at  $T = 2$  K of the magnetic moment of samples a) 2 and b) 3, before and after irradiation. Note the small remaining hysteresis between 2 and 4 T in the irradiated sample 3. The diamagnetic background obtained at 300 K was subtracted from the measured data. The measurements of sample 2 were done in two field directions with similar results within resolution. The direction of the applied field shown in all figures is  $\perp$  [111].

The magnetic moment  $m$  of the diamond samples shown in Figure 1 and 7 was measured with the large surface areas of the samples parallel to the magnetic field applied  $\perp$  [111]. Measurements at other field directions were also done to check for the existence of any magnetic anisotropy. The magnetic moment did not show any anisotropy within error, in agreement with the reported data in the study by Barzola-Quiquia et al.<sup>[26]</sup>

We note that the high sample-temperature stabilized during irradiation is not the reason for the changes we discuss in the following text. To prove this, we show in Figure 1 the magnetization field hysteresis loop at 2 K of sample 4 before and after annealing at 1200 °C in vacuum for 4 h. The field loops indicate that the main field hysteresis does not change significantly after annealing.

The influence of the electron irradiation on the field hysteresis is clearly shown in Figure 7. The field hysteresis is suppressed. The s-like field loop curve obtained for both samples at  $T = 2$  K after irradiation is due exclusively to a PM phase, not SPM, as the measured temperature dependence of the magnetic moment also indicates, see Section 5.2.

## 5.2. Temperature Hysteresis Loops

To further demonstrate that the s-like field loop observed after irradiation, see Figure 7, is related to a PM phase, we discuss the measured temperature dependence before and after

irradiation. Figure 8a shows the magnetic moment of sample 3 before and after irradiation vs inverse temperature obtained at an applied field of 1 T. As discussed in detail in,<sup>[26]</sup> the Curie-like behavior observed at relatively high temperatures, i.e., at  $T > 20$  K, see Figure 8a, does not scale with the applied field as one expects for a PM phase. Its susceptibility clearly increases with the applied field,<sup>[26]</sup> indicating the development of a SPM phase at low temperatures. This SPM phase does not show any hysteresis in field in the measured temperature range, although its s-shape in the field hysteresis loop looks similar to a FM state. The clear hysteresis in the temperature loop, see Figure 8a, has a different origin. In the study by Barzola-Quiquia et al.,<sup>[26]</sup> it has been interpreted as due to a SC contribution added to the SPM one.

After electron irradiation, we observe remarkable changes in the temperature dependence of the magnetic moment, namely:

- The main change after irradiation is observed at  $T < 30$  K,

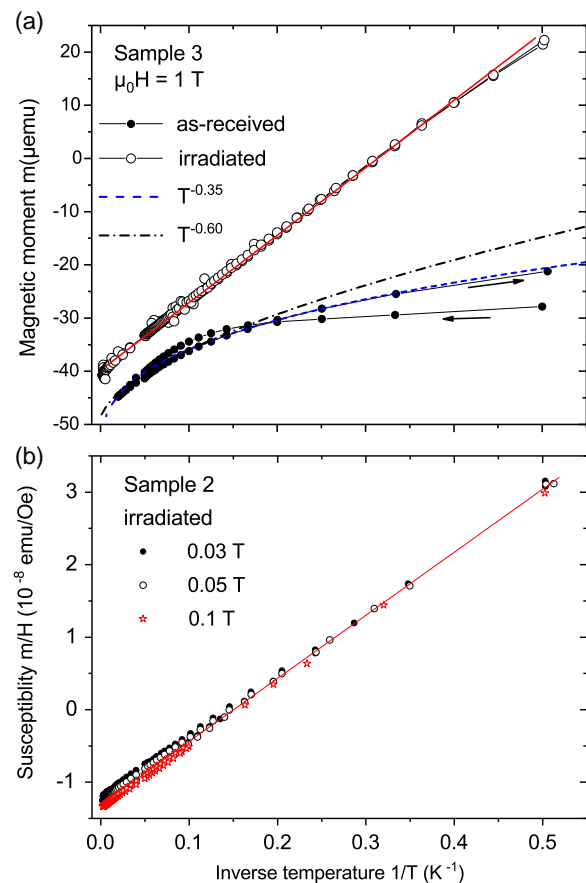


**Figure 8.** a) Magnetic moment versus inverse temperature measured at a constant field of 1 T for sample 3 in the as-received and irradiated states. Note the temperature hysteresis between the ZFC (increasing temperature path) and the FC (decreasing temperature path) states. The dashed line follows  $m(T) = 45T^{-0.35} - 56$  [ $\mu\text{emu}$ ] and the dashed-dotted line  $m(T) = 52T^{-0.6} - 49$  [ $\mu\text{emu}$ ] with  $T$  in K. b) Magnetic susceptibility, defined as the ratio between the magnetic moment and the applied field, versus inverse temperature for sample 2 in the irradiated state at three magnetic fields. No background was subtracted from the raw data. The straight line is a linear fit to the data.



where the large hysteretic contribution is completely suppressed. The magnetic moment shows a Curie-law behavior in the whole temperature range, with a weak tendency to saturation at the lowest measured temperatures at an applied field of 1 T, see Figure 8a, as expected for a PM phase. b) From the slope of  $m$  versus  $1/T$  and assuming a total angular momentum  $J = 1/2$  and  $g_j = 2$  per PM center, we estimate a concentration of  $(40 \pm 5)$  ppm PM centers for sample 3 after irradiation with a fluence of  $1 \times 10^{18} \text{ cm}^{-2}$ . This value can be interpreted as due to the following contributions: one from the C centers with a concentration of  $\approx 10$  ppm, see Table 1, H1a centers of  $\lesssim 5$  ppm concentration and a rest of  $\approx 25$  ppm of magnetic centers due either vacancies and/or lattice defects produced by them. c) The results obtained from sample 2 after irradiation are shown in Figure 8b where the susceptibility versus inverse temperature at three applied fields is plotted. The temperature dependence and the observed scaling with applied field are compatible with a PM phase, see Figure 8b. From the susceptibility slope versus  $1/T$  of sample 2 and after two times higher electron irradiation fluence the calculated density of PM centers is  $(80 \pm 5)$  ppm. It means a factor of four larger than the density of C centers obtained by EPR and IR, see Table 1. This indicates that about 60 ppm of the PM centers measured by the magnetic susceptibility should be related to extra lattice defects induced by the irradiation, with a magnetic moment of the order of  $1 \mu_B$ . d) After an electron irradiation with a fluence that produced a decrease in a factor of two in the C-center concentration (equivalent to some tens of ppm), any anomalous signs of hysteresis in field and temperature are completely absent at  $T \geq 2$  K, within experimental resolution.

### 5.3. Partial Recovery of the Anomalies in the Magnetization After High-Temperature Annealing in Vacuum

In an earlier study, Creedon et al.<sup>[17]</sup> found that the observed suppression of SC of B-doped diamond after a certain fluence of He-ion irradiation, could be partially recovered after annealing the sample in vacuum. Therefore, we annealed some of the samples in vacuum at  $1200^\circ\text{C}$  for 4 h with a 10 h ramp up and down, following the sequence used in.<sup>[17]</sup> Figure 9 shows the difference between the magnetic moment at field cooling (FC) and at ZFC states of sample 3 obtained at constant field of 1 T in the as-received, after irradiation, and after two identical annealing processes. A finite, negative difference in  $m_d = m_{FC} - m_{ZFC}$  is observed at  $5 \text{ K} \lesssim T \lesssim 35 \text{ K}$  in the as-received state, in agreement with the earlier publication.<sup>[26]</sup> An interpretation for this anomalous difference is given in the discussion.

After electron irradiation  $m_d = (0 \pm 1) \mu\text{emu}$  in the whole temperature range, see Figure 9. After the first annealing, a similar behavior as in the as-received state is observed but  $m_d$  starts to be negative at  $T < 10$  K showing the minimum at  $\approx 3$  K (instead of 10 K as in the as-received state). A second annealing slightly increases  $|m_d|$  with a small shift to higher temperatures. The obtained behavior of  $m_d(T)$  after annealing indicates the partial recovering of the regions responsible for the anomalous behavior of the magnetization.

This partial recovering is also observed by measuring the field hysteresis loops after annealing, in particular the field hysteresis

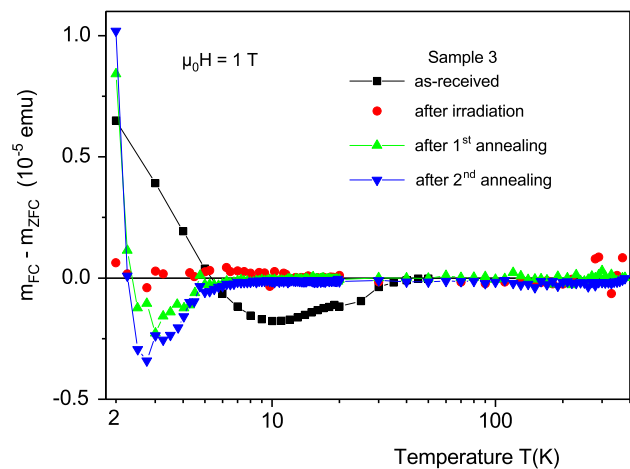


**Figure 9.** Temperature dependence of the difference between the FC and ZFC states  $m_d = m_{FC} - m_{ZFC}$  measured in sample 3 in the as-received, after irradiation and after the first and second annealing treatments at a constant applied field of 1 T.

width. Figure 10 shows the field hysteresis width at a constant field of 3 T versus temperature for the as-received and after the two annealing treatments after irradiation of sample 3. The results indicate that the amplitude of the anomaly in the magnetization partially recovers after annealing, see Figure 10. However, whether a critical temperature is really reduced respect to the one in the as-received state is not so clear because of the different temperature dependences, see Figure 10. An apparent reduction of the superconducting  $T_c$  obtained from transport measurements has been reported after subsequent annealing treatment of a previously He-ion-irradiated B-doped diamond sample.<sup>[17]</sup>

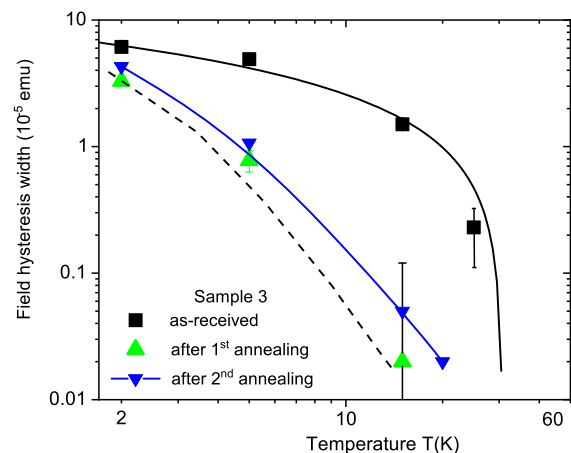


**Figure 10.** Field hysteresis width at a constant field of 3 T measured at different temperatures for sample 3 in the as-received, first and second annealing treatment after electron irradiation. The black line follows the equation  $0.05 - 2.3 \ln(T/T_c)$  with  $T_c = 30$  K. This phenomenological equation was found to satisfactorily describe the critical line of several as-received N-doped diamonds.<sup>[26]</sup> The blue and dashed lines through the data points of the annealed samples are only a guide to the eye.

## 6. Discussion

Pure diamond samples, without N- or B-doping, show no anomalous behavior in the magnetization above 2 K but the usual diamagnetic response. A very weak Curie-like behavior in the magnetic susceptibility below 100 K is observed in some of the “pure” diamond samples, with a temperature irreversibility between the ZFC and FC states more than three orders of magnitude smaller than the irreversibility we measured in N-doped diamond.<sup>[26]</sup> Because the concentration of boron in all diamond crystals presented in this work is below 1 ppm, we can certainly rule out B-doping as responsible for the anomalies in the magnetization.

A correlation between the anomalous maximum in magnetization and the concentration of C centers has been obtained in the study by Barzola-Quiquia et al.<sup>[26]</sup> Also, our results indicate a correlation to the C centers. But this correlation is not a simple one, as the vanishing and recovery of the anomalies and the corresponding C centers concentration for those states indicate, see Table 1.

As emphasized in Section 1, the similarities between the magnetization loops obtained in N-doped diamonds and FM/SC bilayers, see Figure 1, suggest that the anomalous behavior is related to the existence of both, a SC and a SPM phase, as proposed in the original publication. The way to simulate such a rather anomalous field hysteresis is given by the simple superposition of each field-dependent magnetization plus eventually a small diamagnetic background, linear in field. The good fits of the field hysteresis data of the diamond samples (as well as of the bilayers) to this model can be seen in the study by Barzola-Quiquia et al.<sup>[26]</sup> Also the obtained dependence of the fit parameters in temperature supports the used model.

At this point, we would like to give a couple of remarks on the EPR measurements. One would argue that below 30 K and if such a mixture of SC and SPM phases in our samples exists, then we would expect to see a broadening of the EPR line related to the C centers at low temperatures. To check for this effect, we have done additional EPR experiments with samples 1, 2, and 3 at 11 K. A significant line broadening for the signals of the C and NV centers was not observed, in comparison with the room temperature spectra. The main reason for the absence of such a broadening of the EPR C-lines is the following. EPR measures the average response of all C centers, which are distributed through all the sample. From all those regions, only a small part of them have the phases responsible for the huge field (and temperature) hysteresis loops. With our EPR equipment, it is simply not possible to get the signal of such a small amount. Note that, there is always an overlap with the dominating signal from the C centers located all over the remaining parts of the sample.

### 6.1. How Large Would Be a Significant C-Centers Concentration to Trigger Ordering Phenomena in Diamond?

This question is not answered experimentally in the literature. Surprisingly, with exception,<sup>[26]</sup> systematic bulk magnetization measurements of diamond samples with different concentration of P1 or C centers are not apparently published. Because the

purity of diamond crystals nowadays is high and especially magnetic impurities can be quantitatively measured with high resolution (e.g., with PIXE); there are no clear reasons why such measurements were not systematically done in the past.

To estimate the average distance between C centers, we follow a similar procedure as in,<sup>[56]</sup> getting an average distance between C centers  $\langle d \rangle_{C-C} = (2.9 \pm 1.5)$  nm in the diamond matrix for a mean concentration of the order of 50 ppm. Because the concentration of C centers is not homogeneously distributed in the diamond samples, it is quite plausible that clusters with an average smaller distance exist. Is such a distance between C centers in the diamond matrix too large to trigger ordering phenomena, even at low temperatures?

Let us take a look at two recent publications that studied the entanglement between single defect spins<sup>[57]</sup> and NV<sup>-</sup>-N<sup>+</sup> pair center.<sup>[58]</sup> In the first study deterministic entanglement of electron spins over a distance of 10 nm was demonstrated at room temperature. In the second work done in 1b diamond, the authors found that for all NV centers with a neutral N within a distance of 5 nm, an electron can tunnel giving rise to NV<sup>-</sup>-N<sup>+</sup> pairs. Considering these studies, a non-negligible coupling between C centers with an average distance of less than 3 nm does not appear impossible.

A concentration of 50 ppm of C centers is much smaller than the necessary boron concentration ( $\approx 2\%$ ) reported in the literature to trigger the observed superconducting transition in the electrical resistance. As we noted in Section 1, new experimental studies do suggest that the relationship between carrier concentration due to B-doping and the superconducting critical temperature is not as clear. It may well be that the relatively high carrier concentration in those B-doped diamonds is necessary to get percolation, i.e., a superconducting current path between voltage electrodes. But it does not necessarily rule out that localized superconducting grains are formed at lower B concentration.

### 6.2. Granularity

We may ask now, why the superconducting transition is not observed in the electrical resistance in our N-doped diamond samples?<sup>[26]</sup> The reason is the granularity of the C-center distribution; it prevents the percolation of a superconducting path between voltage electrodes when their distance is much larger than the grain size, see Figure 4. This granularity added to the apparently small amount of the total sample mass that shows a superconducting response is the reason why transport measurements are so difficult to perform in these samples.

From the comparison between the absolute magnetic signals in the diamond samples and those measured in oxides bilayers, a rough estimate of the equivalent mass of the SC phase in the N-doped diamond samples gives  $\approx 1$   $\mu\text{g}$ , i.e., the volume of a cube of 70  $\mu\text{m}$  side length.<sup>[26]</sup> This estimate suggests that micrometer large clusters of superconducting C centers should exist in the sample, as the image in Figure 4 shows. Note that, the assumption that all the measured anomalous magnetic signals would come from very few, well localized regions with a very high C-center concentration in the percent region, as in the case of B-doped diamond, does not find support from our IR-absorption images. Also, the clear suppression of the two phases after such a weak and

homogeneous electron irradiation and the thereof decrease in the C-center concentration, speaks against such an assumption. The obtained evidence speaks for a correlation of the observed phenomena with localized clusters of C centers with concentration at least ten times smaller than the reported B concentration in B-doped diamond, see Section 1.1 and references therein.

We note that several experimental details gained from our magnetization results suggest that the SPM phase should emerge simultaneously to the SC one. For example, the anomalous behavior of the difference  $m_d = m_{FC} - m_{ZFC}$ , see Figure 9. We note first that in the case we would have only a superconducting single phase, we expect  $m_d > 0$  at  $T < T_c$ . An interpretation for the anomalous behavior of  $m_d(T)$  has been provided in the study by Barzola-Quiquia et al.<sup>[26]</sup> considering that the samples have both, an SC and an SPM phase. In this case, the anomalously large increase in the magnetic moment  $m_{ZFC}$  is due to the partial field expulsion in the SC regions. In other words, an effective higher field than the applied one enhances the magnetic moment of the SPM phase in the ZFC state and therefore  $m_d < 0$ . At low enough temperatures,  $m_{FC}$  increases and eventually  $m_d > 0$ , as observed. We emphasize that similar results were obtained in FM/SC oxide bilayers, supporting this interpretation.<sup>[26]</sup>

### 6.3. Possible Origin for the Existence of Two Antagonist Phases Within Regions with High C-Centers Concentration

Clustering of C centers could produce a spin glass phase arising from their spin 1/2 character of independent magnetic moments. Following the ideas of the resonating valence bond (RVB) model,<sup>[22,59]</sup> as temperature is reduced the C centers start to be weakly coupled and could form pairwise, antiferromagnetically (AFM) coupled singlets. A certain density of these donors may delocalize, leading to a SC state at low enough temperatures.

There are at least two possible scenarios that could provide an answer to the simultaneous existence of the two phases. The rather conventional possibility is that at low enough temperatures, in our case  $T \lesssim 30$  K, a mixture of paired and unpaired C centers are formed, a spin liquid. The unpaired C centers start to contribute to the magnetic response under an applied magnetic field as a SPM phase, the reason for the s-like field loop contribution without any field hysteresis. An SPM phase, instead of a FM one, is possible only if the spin–spin interaction (inversely proportional to the distance between the spins) is weak enough within the used temperature range.

The successive coupling of the C centers is predicted to be a kind of hierarchical process, which leads to a non-Curie law in the magnetic susceptibility as, for example,  $\chi \propto T^{-\alpha}$ . Such a process has been observed in P-doped Si with  $\alpha \approx 0.6$ .<sup>[60,61]</sup> The FC susceptibility of our diamond samples in the as-received state follows a similar temperature dependence but with  $\alpha \approx 0.35$ , indicating the superposition of a strong diamagnetic response, as expected if a SC phase develops, see Figure 8a. The results in Figure 8a show also that at high enough temperatures most of the C centers depair and contribute as independent PM centers to the magnetic susceptibility.

A less conventional possibility follows from arguments published in the studies by Baskaran and Mareš et al.<sup>[22,62]</sup>: spin–spin interaction is the most robust attractive interaction in this kind of

doped systems, which may operate simultaneously to the electron–phonon interaction to create Cooper pairs. It follows that, unlike s-wave, p-wave superconductors do not necessarily have their Cooper pairs mediated by phonons. We may argue therefore that, instead of a s-wave pairing, a p-wave SC state between the interacting donors could also be possible. In this case the response to an applied magnetic field of a system of p-wave symmetry Cooper pairs could produce a mix response of a SPM together to a field hysteresis loop due to the existence of vortices and/or fluxons in the SC regions. As example, we refer to the theoretical study of the orbital magnetic dynamics in a p-wave superconductor with strong crystal-field anisotropy.<sup>[63]</sup> In this case, the orbital moment of Cooper pairs (the directional order parameter) does not lead to a definite spontaneous magnetization, i.e., no hysteresis as in a SPM phase. Clearly, more experimental evidence tying the possible causes to a consistent, measurable effect is necessary.

### 6.4. What Electron Irradiation Does and Why the Observed Effect Is of Importance

Let us now discuss the effect of the electron irradiation. One main result is that a nominal induced defect concentration  $\approx 50$  ppm, of the order of the concentration of C centers in the as-received state of the samples, eliminates completely the anomalies in the magnetization. It would mean that the two phases, SC and the SPM phases, vanish simultaneously. Considering that most of those produced vacancies diffuse and/or give rise N-related defects, and the correlation found in the study by Barzola-Quiquia et al.,<sup>[26]</sup> it is appropriate to correlate the vanishing of the anomalies after irradiation with the measured decrease in  $\approx 10$ – $40$  ppm of C centers, see Table 1.

Qualitatively, the irradiation effect we found is similar to the vanishing of SC by He ions' irradiation in B-doped diamond.<sup>[17]</sup> This similarity is remarkable because the studies in B-doped diamond show a suppression of SC after producing a vacancy concentration  $\approx 2\%$ , similar to the boron concentration. This result also indicates that in the N-doped samples the SC/SPM regions should be spread in the whole sample and not just at certain localized regions, each with orders of magnitude larger density of C centers. If that were the case, it would be difficult to understand how a change of  $\approx 40$  ppm in the defect concentration (C centers and/or other lattice defects) is enough to suppress the two phases. This experimental result supports the notion that nitrogen doping of diamond is extraordinary, especially because of the low level of doping needed to trigger the observed irreversibilities in the magnetization and at relatively high temperatures.

The suppression of SC in B-doped diamond after He irradiation has been explained assuming that the produced vacancies act as donors, which compensate the holes introduced by the substitutional boron atom.<sup>[17]</sup> Evidently, this argument is not applicable in the case of the N-doped diamond, because nitrogen is already a donor in the diamond matrix.

From our results, we may conclude that one main reason for the vanishing of the responsible phases by electron irradiation is the decrease by  $\approx 50\%$  of the average concentration of C centers, see Table 1. However, would that decrease in the C-center concentration be the only effect, then we would expect to still observe the

two phases, though with less amplitude of the anomalies in the magnetization. This expectation is based on the rather weak dependence of the  $T_c$  on the average concentration of C centers, obtained from eight diamond samples with differences up to a factor of four.<sup>[26]</sup> It means that the irradiation-produced lattice defects strongly affect the interaction between the remaining C centers.

The produced lattice defects through irradiation (H1a centers,<sup>[54]</sup> remaining vacancies<sup>[40]</sup> and other N centers) could affect not only the randomness of the lattice strain, the distribution of the internal electric field and of the covalent bonds that contribute to stabilize the SC phase,<sup>[27]</sup> but also their magnetic moments could have a detrimental role in the coupling between the C centers. If this would be the case, then a distribution of C centers in a diamond lattice with a similar amount of magnetic defects not necessarily would trigger SC but only PM. In fact, the susceptibility results after irradiation indicate that most of the remaining C centers contribute independently to a PM state at all temperatures.

The study by Creedon et al.<sup>[17]</sup> found that a partial recovery of the SC occurs after annealing the He-irradiated B-doped diamond samples. A similar annealing treatment done in our samples also produces the recovery of the anomalies in the magnetization but their magnitude is smaller than in the as-received state at similar temperatures, see Figure 10. Which is actually the effect of annealing? After electron irradiation, annealing at high temperatures and in vacuum reduces only slightly the average concentration of C centers ( $\approx 6\%$ , see Table 1) but increases significantly the homogeneity in their spatial distribution, see Figure 5. Because the total amount of C centers did not change basically after annealing, see Table 1, the partial recovering of the responsible phases after annealing, appears to be related to the clear increase in homogeneity. Our IR results do not indicate that the concentration of H1a centers decreases with annealing.

## 7. Conclusions

Magnetization measurements of electron irradiated N-doped diamond crystals show the suppression of the anomalous irreversible behavior in applied magnetic field and temperature. The suppression occurs after producing a decrease of a few tens of ppm in the concentration of C centers measured by IR absorption and EPR. This is remarkable because of the relatively low density of C centers, stressing the extraordinary role of the C centers in triggering those phenomena in diamond at relatively high temperatures. Spectroscopy methods like ARPES to get information on the changes in the band structure produced by nitrogen would be of high interest. However, it is not clear whether such a technique would be successful using similar samples as we studied here, due to the small amount of mass of the phases that originate the anomalies in the magnetization. We believe that future work should try to study the magnetic and electrical response locally to localize the regions of interest. According to our results, the regions of interest should be all over distributed in the samples and therefore these local studies should have a reasonable chance of success. However, the main problem would be the large measuring scanning time (at a fixed temperature and magnetic field) for the typical areas of the samples studied here.

## Acknowledgements

The authors thank W. Böhlmann for the technical support. P.D.E. thanks G. Baskaran and G. Zhang for fruitful discussions on their work. The studies were supported by the DFG under the grant DFG-ES 86/29-1 and DFG-ME 1564/11-1. The work in Russia was partially funded by Russian Foundation for Basic Research (RFBR) and National Natural Science Foundation of China (NSFC) research project 20-52-53051.

Open Access funding enabled and organized by Projekt DEAL.

## Conflict of Interest

The authors declare no conflict of interest.

## Data Availability Statement

Research data are not shared.

## Keywords

color centers, diamond, magnetism

Received: August 4, 2021

Revised: August 30, 2021

Published online: September 28, 2021

- [1] E. A. Ekimov, V. A. Sidorov, E. D. Bauer, N. N. Mel'nik, N. J. Curro, J. D. Thompson, S. M. Stishov, *Nature* **2004**, 428, 542.
- [2] Y. Takano, M. Nagao, I. Sakaguchi, M. Tachiki, T. Hatano, K. Kobayashi, H. Umezawa, H. Kawarada, *Appl. Phys. Lett.* **2004**, 85, 2851.
- [3] Y. Takano, M. Nagao, T. Takenouchi, H. Umezawa, I. Sakaguchi, M. Tachiki, H. Kawarada, *Diamond Relat. Mater.* **2005**, 14, 1936 [Proc. of the 10th Int. Conf. on New Diamond Science and Technology (ICNDST-10)].
- [4] T. Yokoya, T. Nakamura, T. Matsushita, T. Muro, Y. Takano, M. Nagao, T. Takenouchi, H. Kawarada, T. Oguchi, *Nature* **2005**, 438, 647.
- [5] N. Murata, J. Haruyama, J. Reppert, A. M. Rao, T. Koretsune, S. Saito, M. Matsudaira, Y. Yagi, *Phys. Rev. Lett.* **2008**, 101, 027002.
- [6] H. Okazaki, T. Wakita, T. Muro, T. Nakamura, Y. Muraoka, T. Yokoya, S.-I. Kurihara, H. Kawarada, T. Oguchi, Y. Takano, *Appl. Phys. Lett.* **2015**, 106, 052601.
- [7] A. Bhaumik, R. Sachan, S. Gupta, J. Narayan, *ACS Nano* **2017**, 11, 11915.
- [8] G. Zhang, S. Turner, E. A. Ekimov, J. Vanacken, M. Timmermans, T. Samuely, V. A. Sidorov, S. M. Stishov, Y. Lu, B. Deloof, B. Goderis, G. Van Tendeloo, J. Van de Vondel, V. V. Moshchalkov, *Adv. Mater.* **2014**, 26, 2034.
- [9] V. D. Blank, B. A. Kulnitskiy, I. A. Perezhogin, S. A. Terentiev, S. A. Nosukhin, M. S. Kuznetsov, *Mater. Res. Express* **2014**, 1, 035905.
- [10] T. Yamamoto, K. Natsui, Y. Einaga, *Photon-Working Switches*, Springer, Japan **2017**, ch. 14.
- [11] V. Blank, S. Buga, V. Bormashov, V. Denisov, A. Kirichenko, V. Kulbachinskii, M. Kuznetsov, V. Kytin, G. Kytin, S. Tarelkin, S. Terentiev, *Europhys. Lett.* **2014**, 108, 67014.
- [12] S. N. Polyakov, V. N. Denisov, B. N. Mavrin, A. N. Kirichenko, M. S. Kuznetsov, S. Y. Martyushov, S. A. Terentiev, V. D. Blank, *Nanoscale Res. Lett.* **2016**, 11, 11.



- [13] G. Zhang, S. D. Janssens, J. Vanacken, M. Timmermans, J. Vack, G. W. Ataklti, W. Decelle, W. Gillijns, B. Goderis, K. Haenen, P. Wagner, V. V. Moshchalkov, *Phys. Rev. B* **2011**, *84*, 214517.
- [14] G. Zhang, T. Samuely, J. Kačák, E. A. Ekimov, J. Li, J. Vanacken, P. Szabó, J. Huang, P. J. Pereira, D. Cerbu, V. V. Moshchalkov, *Phys. Rev. Appl.* **2016**, *6*, 064011.
- [15] G. Zhang, J. Kačák, Z. Wang, R. Zulkharnay, M. Marcin, X. Ke, S. Chiririev, V. Adashkevich, P. Szabó, Y. Li, P. Samuely, V. V. Moshchalkov, P. W. May, H.-G. Rubahn, *Phys. Rev. Appl.* **2019**, *12*, 064042.
- [16] J. Bousquet, T. Klein, M. Solana, L. Saminadayar, C. Marcenat, E. Bustarret, *Phys. Rev. B* **2017**, *95*, 161301.
- [17] D. L. Creedon, Y. Jiang, K. Ganesan, A. Stacey, T. Kageura, H. Kawarada, J. C. McCallum, B. C. Johnson, S. Prawer, D. N. Jamieson, *Phys. Rev. Appl.* **2018**, *10*, 044016.
- [18] V. Heera, R. Höhne, O. Ignatchik, H. Reuther, P. Esquinazi, *Diamond Relat. Mater.* **2008**, *17*, 383.
- [19] L. H. Willems van Beveren, R. Liu, H. Bowers, K. Ganesan, B. C. Johnson, J. C. McCallum, S. Prawer, *J. Appl. Phys.* **2016**, *119*, 223902.
- [20] N. Tsubouchi, S. Shikata, *Nucl. Instrum. Methods Phys. Res. Sect. B* **2012**, *286*, 303 [Proc. of the Sixteenth Int. Conf. on Radiation Effects in Insulators (REI)].
- [21] N. Tsubouchi, M. Ogura, Y. Horino, H. Okushi, *Appl. Phys. Lett.* **2006**, *89*, 012101.
- [22] G. Baskaran, *Sci. Technol. Adv. Mater.* **2008**, *9*, 044104.
- [23] G. Zhang, T. Samuely, Z. Xu, J. K. Jochum, A. Volodin, S. Zhou, P. W. May, O. Onufrienko, J. Kačmarčák, J. A. Steele, J. Li, J. Vanacken, J. Vack, P. Szabó, H. Yuan, M. B. J. Roeffaers, D. Cerbu, P. Samuely, J. Hofkens, V. V. Moshchalkov, *ACS Nano* **2017**, *11*, 5358.
- [24] G. Zhang, T. Samuely, N. Iwahara, J. Kačmarčák, C. Wang, P. W. May, J. K. Jochum, O. Onufrienko, P. Szabó, S. Zhou, P. Samuely, V. V. Moshchalkov, L. F. Chibotaru, H.-G. Rubahn, *Sci. Adv.* **2020**, *6*, 20.
- [25] S. Talapatra, P. G. Ganesan, T. Kim, R. Vajtai, M. Huang, M. Shina, G. Ramanath, D. Srivastava, S. C. Deevi, P. M. Ajayan, *Phys. Rev. Lett.* **2005**, *95*, 097201.
- [26] J. Barzola-Quiquia, M. Stiller, P. D. Esquinazi, A. Molle, R. Wunderlich, S. Pezzagna, J. Meijer, W. Kossack, S. Buga, *Sci. Rep.* **2019**, *9*, 8743.
- [27] C. Liu, X. Song, Q. Li, Y. Ma, C. Chen, *Phys. Rev. Lett.* **2020**, *124*, 147001.
- [28] E. Tang, L. Fu, *Nat. Phys.* **2014**, *10*, 964.
- [29] N. Y. Fogel, A. S. Pokhila, Y. V. Bomze, A. Y. Sipatov, A. I. Fedorenko, R. I. Shekhter, *Phys. Rev. Lett.* **2001**, *86*, 512.
- [30] N. Y. Fogel, E. I. Buchstab, Y. V. Bomze, O. I. Yuzepovich, M. Y. Mikhailov, A. Y. Sipatov, E. A. Pashitskii, R. I. Shekhter, M. Jonson, *Phys. Rev. B* **2006**, *73*, 161306.
- [31] F. Muntyanua, A. Gilewski, K. Nenkov, A. Zaleski, V. Chistol, *Solid State Commun.* **2008**, *147*, 183.
- [32] N. B. Kopnin, M. Ijäs, A. Harju, T. T. Heikkilä, *Phys. Rev. B* **2013**, *87*, 140503.
- [33] W. A. Muñoz, L. Covaci, F. Peeters, *Phys. Rev. B* **2013**, *87*, 134509.
- [34] B. Pamuk, J. Baima, F. Mauri, M. Calandra, *Phys. Rev. B* **2017**, *95*, 075422.
- [35] A. Ballestar, J. Barzola-Quiquia, T. Scheike, P. Esquinazi, *New J. Phys.* **2013**, *15*, 023024.
- [36] Y. Cao, V. Fatemi, S. Fang, K. Watanabe, T. Taniguchi, E. Kaxiras, P. Jarillo-Herrero, *Nature* **2018**, *556*, 43.
- [37] S. C. Lawson, D. Fisher, D. C. Hunt, M. E. Newton, *J. Phys.: Condens. Matter* **1998**, *10*, 6171.
- [38] V. M. Acosta, E. Bauch, M. P. Ledbetter, C. Santori, K.-M. C. Fu, P. E. Barclay, R. G. Beausoleil, H. Linget, J. F. Roch, F. Treussart, S. Chemerisov, W. Gawlik, D. Budker, *Phys. Rev. B* **2009**, *80*, 115202.
- [39] M. Capelli, A. Heffernan, T. Ohshima, H. Abe, J. Jeske, A. Hope, A. Greentree, P. Reineck, B. Gibson, *Carbon* **2019**, *143*, 714.
- [40] B. Campbell, A. Mainwood, *Phys. Status Solidi A* **2000**, *181*, 99.
- [41] Y. Mindarava, R. Blinder, C. Laube, W. Knolle, B. Abel, C. Jentgens, J. Isoya, J. Scheuer, J. Lang, I. Schwartz, B. Naydenov, F. Jelezko, *Carbon* **2020**, *170*, 182.
- [42] M. Newton, B. Campbell, D. Twitchen, J. Baker, T. Anthony, *Diamond Relat. Mater.* **2002**, *11*, 618 [12th European Conf. on Diamond, Diamond-Like Materials, Carbon Nanotubes, Nitrides & Silicon Carbide].
- [43] J. Loubser, J. van Wyk, *Rep. Prog. Phys.* **1978**, *41*, 1201.
- [44] A. R. Lang, M. Moore, A. P. W. Makepeace, W. Wierczowski, C. M. Welbourn, *Philos. Trans. R. Soc. London, Ser. A* **1991**, *337*, 497.
- [45] S. R. Boyd, I. Kiflawi, G. S. Woods, *Philos. Mag. B* **1995**, *72*, 351.
- [46] T. Hainschwang, E. Fritsch, L. Massi, U. B. Rondeau, F. Notari, *J. Appl. Spectrosc.* **2012**, *79*, 737.
- [47] N. Kazuchits, M. Rusetzky, V. Kazuchits, A. Zaitsev, *Diamond Relat. Mater.* **2016**, *64*, 202.
- [48] A. T. Collins, I. Kiflawi, *J. Phys.: Condens. Matter* **2009**, *21*, 364209.
- [49] P. R. Briddon, R. Jones, M. I. Heggie, *Int. Conf. New Diamond Science and Technology, MRS Proc.* **1991**, p. 63.
- [50] A. T. Collins, G. S. Woods, *Philos. Mag. B* **1982**, *46*, 77.
- [51] G. S. Woods, A. T. Collins, *J. Phys. C: Solid State Phys.* **1982**, *15*, L949.
- [52] I. Kiflawi, A. Mainwood, H. Kanda, D. Fisher, *Phys. Rev. B* **1996**, *54*, 16719.
- [53] J. P. Goss, P. R. Briddon, S. Papagiannidis, R. Jones, *Phys. Rev. B* **2004**, *70*, 235208.
- [54] Y. Babich, B. Feigelson, A. Chepurov, *Diamond Relat. Mater.* **2016**, *69*, 8.
- [55] M. W. Dale, Ph. D. Thesis, Department of Physics, University of Warwick, **2015**, <http://wrap.warwick.ac.uk/80044>.
- [56] J. Henshaw, D. Pagliero, P. R. Zangara, M. B. Franzoni, A. Ajoy, R. H. Acosta, J. A. Reimer, A. Pines, C. A. Meriles, *Proc. Natl. Acad. Sci. USA*, **2019**, *116*, 18334.
- [57] F. Dolde, I. Jakobi, B. Naydenov, N. Zhao, S. Pezzagna, C. Trautmann, J. Meijer, P. Neumann, F. Jelezko, J. Wrachtrup, *Nat. Phys.* **2013**, *9*, 139.
- [58] N. B. Manson, M. Hedges, M. S. J. Barson, R. Ahlefeldt, M. W. Doherty, H. Abe, T. Ohshima, M. J. Sellars, *New J. Phys.* **2018**, *20*, 113037.
- [59] P. W. Anderson, *Science* **1987**, *235*, 1196.
- [60] M. A. Paalanen, J. E. Graebner, R. N. Bhatt, S. Sachdev, *Phys. Rev. Lett.* **1988**, *61*, 597.
- [61] M. Lakner, H. V. Löhneysen, A. Langenfeld, P. Wölfe, *Phys. Rev. B* **1994**, *50*, 17064.
- [62] J. Mareš, P. Hubík, J. Křištofik, M. Nesladek, *Sci. Technol. Adv. Mater.* **2008**, *9*, 044101.
- [63] V. Braude, E. B. Sonin, *Phys. Rev. B* **2006**, *74*, 064501.